Generation and Direct Detection of Broadband Mesoscopic Polarization-Squeezed Vacuum

Timur Iskhakov,[1] Maria V. Chekhova,[1,2] and Gerd Leuchs[2,3]

[1]*Department of Physics, M. V. Lomonosov Moscow State University, Leninskie Gory, 119992 Moscow, Russia*
[2]*Max Planck Institute for the Science of Light, Günther-Scharowsky-Straße 1/Bau 24, 91058 Erlangen, Germany*
[3]*University Erlangen-Nürnberg, Staudtstrasse 7/B2, 91058 Erlangen, Germany*

Using a traveling-wave optical parametric amplifier with two orthogonally oriented type-I BBO crystals pumped by picosecond pulses, we generate vertically and horizontally polarized squeezed vacuum states within a broad frequency-angular range. Depending on the phase between these states, fluctuations in one or another Stokes parameter are suppressed below the shot-noise limit. Because of the large number of photon pairs produced, no local oscillator is required, and 3 dB squeezing is observed by means of direct detection.

PACS numbers: 42.50.Lc, 42.50.Dv, 42.65.Yj

Squeezed light is the basic resource for continuous-variable quantum communication and computation [1]. Nowadays, the techniques of generating squeezed light are well developed and include $\chi^{(3)}$ interactions in fibers [2] and $\chi^{(2)}$-based optical parametric amplifiers (OPAs), seeded [3,4] or not seeded [5], cavity-based [6] or single-pass [7]. Squeezed light, as a rule, is detected using a local oscillator or, in the case of bright two-mode squeezing, also by direct detection. More advanced techniques of measurement include Wigner-function tomography [8] and polarization tomography [9,10].

In quantum optics of both discrete and continuous variables, a special role is played by squeezed vacuum state. It is the state generated at the output of an unseeded OPA [11]. At low parametric gain, it is known as biphoton light [12], while at high gain it manifests quadrature squeezing [11]. For any parametric gain, squeezed vacuum is nonclassical since it contains only even photon-number states [13].

In particular, two-mode squeezed vacuum generated at the output of an unseeded two-mode OPA [14] has such an important advantage as perfect two-mode squeezing: regardless of the parametric gain, the photon-number difference for the two modes does not fluctuate. Two-mode squeezed vacuum generated in a single-pass OPA is especially interesting: first, because its correlations are not reduced by the cavity losses and, second, because it has a rich broadband, i.e., multimode, frequency and angular spectrum, which can be used for quantum information protocols in higher-dimensional Hilbert spaces. However, because of the difficulties in producing and detecting such states, there are only a few reports on the direct detection of broadband squeezed vacuum, and all of them show only a small degree of squeezing [15–18].

In this Letter, we achieve a considerable degree of two-mode broadband squeezing by combining two coherent strongly pumped single-pass type-I OPAs, which generate squeezed vacua in two orthogonal polarization modes. This creates a squeezed vacuum with the variance of some

Stokes observable suppressed below the shot-noise level, which is determined by the mean number of photons. The latter, coinciding with the zeroth Stokes parameter S_0, gives the variance of any Stokes observable for a coherent beam with the same mean photon number and with any polarization. This special type of two-mode squeezing is often termed polarization squeezing [19], and the state can be called polarization-squeezed vacuum. Note that this definition of polarization squeezing differs from the more commonly used one [20,21], where the modulus of some Stokes observable mean value is put between the variances of the other two Stokes observables, $\mathrm{Var}(S_i) < |\langle S_j \rangle| < \mathrm{Var}(S_k)$, $i, j, k = 1, 2, 3$. This type of polarization squeezing is similar to quadrature squeezing rather than two-mode squeezing. However, both types of polarization squeezing are essentially nonclassical.

In our setup (Fig. 1), two 1-mm BBO crystals with the optic axes oriented in orthogonal (vertical and horizontal) planes were placed into the beam of a Nd:YAG laser third harmonic (wavelength $\lambda_p = 355$ nm). The fundamental and second-harmonic radiation of the laser was eliminated using a prism and a UV filter. The pump pulse width was 17 ps, the repetition rate 1 kHz, and the mean power up to 120 mW. The pump was focused into the crystals by either a lens with focal length 100 cm, which resulted in a beam
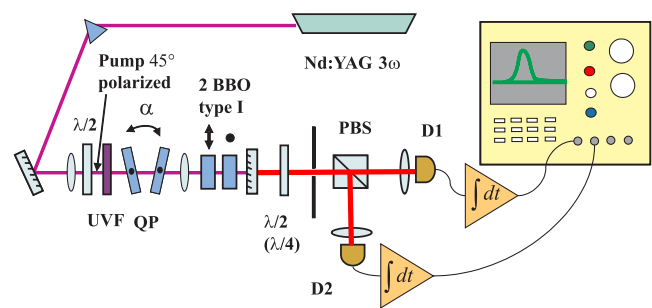
FIG. 1 (color online). Experimental setup. UVF, UV filter; QP, quartz plates; PBS, polarizing beam splitter; D1 and D2, detectors.

waist of 70 μm, or with a telescope, providing a softer focusing (beam waist about 500 μm). Using a half wave plate (HWP), we aligned the pump polarization to be at 45° to the planes of the crystals' optic axes. The crystals were aligned for type-I collinear frequency-degenerate phase matching. After the crystals, the pump radiation was cut off by two dichroic mirrors, having high reflection for the pump and 98.5% transmission for down-converted radiation. The detection part of the setup, including a polarizing beam splitter, a HWP or a quarter wave plate (QWP), and two detectors, provided a standard Stokes measurement. With a HWP oriented at 22.5°, the difference of the detectors' signals corresponded to the second Stokes observable S_2, while with a QWP oriented at 45°, the same measurement provided S_3. All surfaces of the optic elements had a standard broadband antireflection coating. The angular spectrum of the detected light was restricted by an aperture to be 0.8°, and the wavelength range was only restricted by the phase matching and was 130 nm broad, with the central wavelength 709 nm. The detectors were Hamamatsu S3883 p-i-n diodes followed by pulsed charge-sensitive amplifiers [22] based on Amptek A250 and A275 chips, with peaking time 2.77 μs. They had a quantum efficiency of 90% and electronic noise equivalent to 180 electrons/pulse rms. At their outputs, they produced pulses of a given shape, with the duration 8 μs and the amplitude proportional to the integral number of photons per light pulse. The phase between the states generated in the two crystals could be varied by tilting two quartz plates with thicknesses $l_1 = 532$ μm and $l_2 = 523$ μm, placed into the pump beam and having the optic axes oriented vertically.

The output signals of the detectors were measured by means of an analog-digital card integrating the electronic pulses over time. The resulting integrals coincided, up to the amplification factor A, with the photon numbers incident on the detectors during a light pulse. The amplification factors for detectors 1 and 2 were independently calibrated to be $A_1 = 9.96 \times 10^{-3}$ nV s/photon and $A_2 = 1.107 \times 10^{-2}$ nV s/photon. The difference between the detectors' amplification factors was eliminated numerically, by multiplying the result of the measurement for detector 2 by a factor of 0.9–0.92, depending on the alignment. As a result, the output signals of the detectors were balanced to an accuracy of 0.1%. From the data set obtained for 30 000 pulses, mean photon numbers per pulse were measured, as well as the variances of the photon-number difference and photon-number sum for the two detectors. Since the electronic noise was comparable to the shot-noise level, it had to be subtracted. The shot-noise level was measured independently, using a shot-noise limited source [23], and corresponded to a standard deviation of about 250 photons per pulse. The degree of two-mode squeezing was characterized by the noise reduction factor (NRF) [3,15] defined as the ratio of the photon-number difference variance to the mean photon-number sum,

$$\mathrm{NRF} = \frac{\mathrm{Var}(N_1 - N_2)}{\langle N_1 + N_2 \rangle}. \tag{1}$$

The dependence of the detector output signal on the input pump power P is shown in Fig. 2. The measurement was made for a 10 nm-wide band selected by means of an interference filter, and the collection angle of 0.4° selected by an aperture. With the pump focused tightly (using a lens with focal length 100 cm), the dependence is strongly nonlinear [Fig. 2(a)], and by fitting it with the well-known expression for a single-pass OPA output [11],

$$N = m\sinh^2\Gamma, \tag{2}$$

with m denoting the number of modes and the parametric gain scaling as square root of the pump power, $\Gamma = \kappa\sqrt{P}$, κ and m being the fitting parameters, we estimate the highest parametric gain achieved in our measurement as $\Gamma = 3.4$. With soft focusing, by means of a telescope, the $N(P)$ dependence is much less nonlinear [Fig. 2(b)], and the highest gain achieved is only 0.8. From the gain values we see that the number of photons per mode ranges between zero and a hundred; i.e., we are in the regime of mesoscopic twin beams [24]. At the same time, the largest total number of photons per pulse is about 4000 for tight focusing and about 1500 for soft focusing. Without the interference filter, photon numbers per pulse are about 1 order of magnitude higher.

Figure 3 shows the variances of the second and the third Stokes operators measured versus the delay introduced by the two quartz plates between the vertically and horizontally polarized components of the pump beam. The measurement was performed at $\Gamma \approx 0.3$, with the 80 mW pump beam softly focused into the crystals. At the phase delay equal to π, squeezing was obtained in the S_2 Stokes observable, while S_3 was antisqueezed. At zero phase delay, the squeezed Stokes observable was S_3. At the same time, the observable S_1 was always antisqueezed. This behavior is clear from the following simple considerations: the states generated at the outputs of the two crystals consist of horizontally and vertically polarized photon pairs, $|HH\rangle$ and $|VV\rangle$. Because of quantum interference, they become orthogonally polarized pairs. In particular, the sum $|HH\rangle + |VV\rangle$ gives two pairs of right- and left-circularly polarized photons, $|RL\rangle$, while the differ-
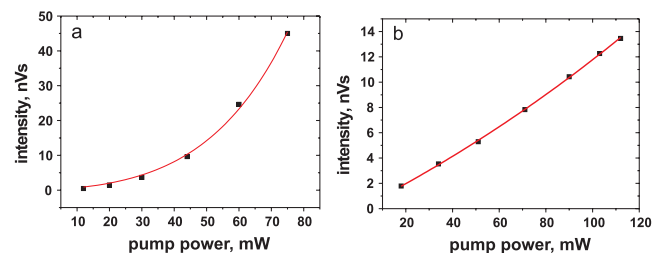
FIG. 2 (color online).   Dependence of the OPA output on the pump power for the beam waist 70 μm (a) and 500 μm (b). Solid lines show a fit with Eq. (2), $m = 34$ (a) and $m = 1400$ (b).
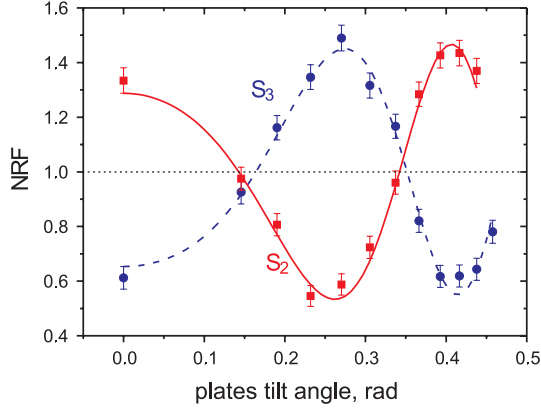
FIG. 3 (color online).   NRF in S_2 (squares, solid line) and S_3 (circles, dashed line) depending on the quartz plates tilt.

ence, $|HH\rangle - |VV\rangle$, gives two pairs of diagonally and antidiagonally polarized photons, $|AD\rangle$. Therefore, the π phase delay between the squeezed vacuum fields generated in the two crystals will lead to a state with suppressed fluctuations in the second Stokes operator, while for the case of the zero phase delay, the state will be squeezed in the third Stokes operator. Note that the mean values of all Stokes observables $\langle S_i \rangle$, $i = 1, 2, 3$ are equal to zero; the state is unpolarized in the "classical optics" sense but polarized in second- and higher-order moments. Indeed, rotation of the HWP or QWP in our measurement setup caused less than 7% variation of the mean signals in both detectors. It is known that mixed states typically can have this property. But there are also pure states with all $\langle S_i \rangle = 0$, e.g., when each of the two polarization modes is in a single-photon state, or the case presented here. This property is called "hidden polarization" [19,20,25] and led to the introduction of various definitions for the degree of polarization [20,26].

A rigorous calculation can be made in the framework of the Heisenberg approach. Denoting the photon creation operators in the horizontal and vertical polarization modes as $a_h^\dagger$ and $a_v^\dagger$, we can write the OPA Hamiltonian as the sum of the Hamiltonians for the two crystals,

$$\hat{H} = G[(a_h^\dagger)^2 + e^{i\phi}(a_v^\dagger)^2] + \text{H.c.,} \qquad (3)$$

where G is proportional to the pump field amplitude and ϕ is the phase delay introduced between the vertical and horizontal pump components. Then the Hamiltonian (3) can be expressed via photon creation operators in orthogonal elliptically polarized modes with the axes of the ellipses oriented at $\pm 45°$, $a_\phi^\dagger \equiv 1/\sqrt{2}(a_h^\dagger + ie^{i\phi/2}a_v^\dagger)$ and $b_\phi^\dagger \equiv 1/\sqrt{2}(a_h^\dagger - ie^{i\phi/2}a_v^\dagger)$ [27]:

$$\hat{H} = 2Ga_\phi^\dagger b_\phi^\dagger + \text{H.c.} \qquad (4)$$

From the form of the Hamiltonian it is clear that the output state has perfectly correlated fluctuations in modes corresponding to the operators a_ϕ, b_ϕ. The mean values

and variances of all Stokes operators can be calculated using the Bogoliubov transformations following from the Hamiltonian (4):

$$a_\phi = Ua_{0\phi} + Vb_{0\phi}^\dagger, \qquad b_\phi = Ub_{0\phi} + Va_{0\phi}^\dagger, \qquad (5)$$

where $U = \cosh\Gamma$ and $V = \sinh\Gamma$, Γ is dimensionless gain proportional to G, and $a_{0\phi}, b_{0\phi}$ are the input (vacuum) photon annihilation operators. Losses in the optical elements and nonunity quantum efficiencies of the detectors can be taken into account in the usual way, by introducing a beam splitter in front of each detector, with the amplitude transmission coefficient $\sqrt{\eta}$ and the amplitude reflection coefficient $\sqrt{1 - \eta}$.

Variances of the Stokes operators $\hat{S}_2 \equiv a_h^\dagger a_v + a_v^\dagger a_h$ and $\hat{S}_3 \equiv -i(a_h^\dagger a_v - a_v^\dagger a_h)$ are found by passing to a_ϕ, b_ϕ operators, then applying transformations (5), and then averaging the second-order moments over the vacuum state. The result, with an account for losses η, is

$$\frac{\text{Var}(S_2)}{2\eta V^2} = (1 - \eta)\sin^2\frac{\phi}{2} + (2\eta U^2 + 1 - \eta)\cos^2\frac{\phi}{2},$$
$$\frac{\text{Var}(S_3)}{2\eta V^2} = (1 - \eta)\cos^2\frac{\phi}{2} + (2\eta U^2 + 1 - \eta)\sin^2\frac{\phi}{2}. \qquad (6)$$

Since the total number of registered photons is $\langle S_0 \rangle = 2\eta V^2$, the left-hand sides of Eqs. (6), according to Eq. (1), give the NRF values for the $\hat{S}_2$ and $\hat{S}_3$ Stokes operators. In the low-gain limit (as is the case for the above-described measurement), $U \approx 1$, and Eqs. (6) become

$$\text{NRF}(S_2) = 1 + \eta\cos\phi, \qquad \text{NRF}(S_3) = 1 - \eta\cos\phi. \quad (7)$$

Equations (7) were used to fit the data shown in Fig. 3, taking into account the approximate relation between the tilt angle of the plates α and the phase $\phi = \phi_0 + 2\pi(l_1 + l_2)(n_o - n_e)[\lambda_p \cos\{\arcsin(2\sin\alpha/(n_o + n_e))\}]^{-1}$, where $n_{o,e}$ are the ordinary and extraordinary refractive indices of quartz. The only fitting parameters being the efficiency η and the initial phase delay ϕ_0, the theoretical dependence is in a good agreement with the experimental data. The resulting quantum efficiency is found to be $\eta = 0.45$, which is considerably less than we expected from the values of the detectors' quantum efficiencies and the optical losses (about 7%).

However, in our experimental scheme there is one more source of losses. Because the nonlinear crystals are placed in series in the pump beam, squeezed vacuum generated in the first crystal has to pass through the second crystal. As it was shown in Ref. [28] for the case of two-photon light, the desired state is only produced in the central part of the frequency-angular spectrum. The state produced at the "slopes," due to the group-velocity dispersion and optical anisotropy, is a different one. In our case the angular bandwidth is restricted by the aperture, but the frequency spectrum contains the whole band allowed by phase matching. If the crystals are aligned to produce, for instance,
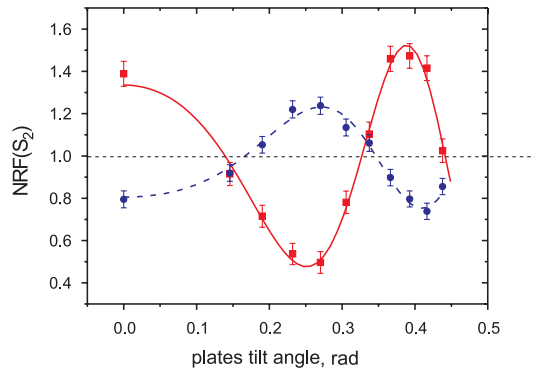
FIG. 4 (color online).   NRF in S_2 versus quartz plates tilt for degenerate (squares) and nondegenerate (circles) phase matching.

S_2-squeezed state at the central wavelength (709 nm), the state at the slopes will be S_3 squeezed and antisqueezed in S_2. According to our numerical calculation, the fraction of the ''correct'' state for the case of degenerate phase matching is 0.71. This explains the low degree of noise suppression in our experiment. The effect of group-velocity dispersion in the second crystal reduces the degree of squeezing even more drastically in the case of nondegenerate phase matching. For instance, for phase matching at 650 and 780 nm, numerical calculation shows that the fraction of the squeezed state in the bandwidth is only 0.52. To test this in the experiment, we measured the S_2 variance for two cases: the crystals aligned for degenerate phase matching and the crystals aligned for phase matching at wavelengths 650 and 780 nm (Fig. 4). While in the first case the NRF falls below 0.5, in the second one its minimal value is 0.75. Note that the interference phase is also changed in the degenerate regime, because of the tilt of the crystals.

We stress that this effect is not inevitable and is only present in configurations where two crystals are placed one after another. A setup with a Mach-Zehnder interferometer [27,29], for instance, is free from this drawback.

In conclusion, we report on a source of broadband twin beams (squeezed vacuum) covering the wavelength range from 650 to 780 nm and the angular range up to 0.8°. The source is a mesoscopic one, providing a number of photons per mode of up to 100. Because of its highly multimode character, the resulting number of photons per pulse is up to 5×10^5. Polarization properties of the produced state reveal ''hidden polarization'' effect: depending on the polarization of the pump beam, the output state has fluctuations in either S_2 or S_3 Stokes observables squeezed 50% below the shot-noise level. To the best of our knowledge, this is the first report on such a high degree of squeezing observed via direct detection of twin beams from a single-pass OPA.

[1] H.-A. Bachor and T. C. Ralph, *A Guide to Experiments in Quantum Optics* (Wiley-VCH, Weinheim, 2004), 2nd ed.
[2] R. M. Shelby *et al.*, Phys. Rev. Lett. **57**, 691 (1986); J. Heersink *et al.*, Phys. Rev. A **68**, 013815 (2003); J. Heersink *et al.*, Opt. Lett. **30**, 1192 (2005).
[3] O. Aytur, P. Kumar, Phys. Rev. Lett. **65**, 1551 (1990).
[4] D. T. Smithey *et al.*, Phys. Rev. Lett. **69**, 2650 (1992).
[5] A. Heidmann *et al.*, Phys. Rev. Lett. **59**, 2555 (1987).
[6] L.-A. Wu *et al.*, Phys. Rev. Lett. **57**, 2520 (1986); J. Gao *et al.*, Opt. Lett. **23**, 870 (1998).
[7] J. A. Levenson *et al.*, Quantum Semiclass. Opt. **9**, 221 (1997); T. Hirano *et al.*, Opt. Lett. **30**, 1722 (2005).
[8] K. Vogel and H. Risken, Phys. Rev. A **40**, 2847 (1989); D. T. Smithey *et al.*, Phys. Rev. Lett. **70**, 1244 (1993).
[9] V. P. Karassiov and A. V. Masalov, J. Opt. B **4**, S366 (2002); P. A. Bushev *et al.*, Opt. Spectrosc. **91**, 526 (2001).
[10] Ch. Marquardt *et al.*, Phys. Rev. Lett. **99**, 220401 (2007).
[11] L. Mandel and E. Wolf, *Optical Coherence and Quantum Optics* (Cambridge University Press, Cambridge, England, 1995).
[12] D. N. Klyshko, *Photons and Nonlinear Optics* (Gordon and Breach, New York, 1988).
[13] Despite its name, squeezed vacuum can have very large mean photon number; see Eq. (2).
[14] S. L. Braunstein, Phys. Rev. A **71**, 055801 (2005).
[15] O. Jedrkiewicz *et al.*, Phys. Rev. Lett. **93**, 243601 (2004).
[16] M. Bondani *et al.*, Phys. Rev. A **76**, 013833 (2007).
[17] G. Brida *et al.*, J. Mod. Opt. (to be published).
[18] T. Sh. Iskhakov *et al.*, JETP Lett. **88**, 660 (2008).
[19] V. P. Karassiov and A. V. Masalov, Opt. Spectrosc. **74**, 551 (1993); P. Usachev *et al.*, Opt. Commun. **193**, 161 (2001).
[20] A. S. Chirkin, A. A. Orlov, and D. Yu. Paraschuk, Quantum Electron. **23**, 870 (1993); A. P. Alodjants, S. M. Arakelian, and A. S. Chirkin, JETP **81**, 34 (1995).
[21] J. Heersink *et al.*, Phys. Rev. A **68**, 013815 (2003).
[22] H. Hansen *et al.*, Opt. Lett. **26**, 1714 (2001).
[23] As a shot-noise limited source, we used the first harmonic of the pump laser attenuated to intensities at which the variance of the difference signal for balanced detectors scaled linearly with the mean intensity.
[24] J. Perina *et al.*, Phys. Rev. A **76**, 043806 (2007).
[25] D. N. Klyshko, Phys. Lett. A **163**, 349 (1992).
[26] V. P. Karassiov, J. Phys. A **26**, 4345 (1993); D. N. Klyshko, JETP **84**, 1065 (1997); A. Luis, Phys. Rev. A **66**, 013806 (2002); G. Björk *et al.*, Proc. SPIE Int. Soc. Opt. Eng. **4750**, 25 (2002); A. B. Klimov *et al.*, Phys. Rev. A **72**, 033813 (2005).
[27] A. V. Burlakov *et al.*, Phys. Rev. A **64**, 041803(R) (2001).
[28] G. Brida *et al.*, Phys. Rev. A **76**, 053807 (2007).
[29] M. Fiorentino and R. G. Beausoleil, Opt. Express **16**, 20 149 (2008).